American Mineralogist, Volume 74, pages 411–421, 1989

Cation ordering in Ni-Mg olivines

G. Ottonello

Dipartimento di Scienze della Terra, Università di Cagliari, Via Trentino 5, 09100 Cagliari, Italy, and
Istituto di Geocronologia e Geochimica Isotopica del C.N.R., Via Cardinale Maffi, 36, 56100 Pisa, Italy

A. Della Giusta, G. M. Molin

Dipartimento di Mineralogia e Petrologia, Università di Padova, Corso Garibaldi 37, 35100 Padova, Italy

Abstract

Single-crystal X-ray structure refinements of crystals with variable compositions in the Ni_2SiO_4-Mg_2SiO_4 join indicate substantial deviations from Vegard's law, primarily in their anomalous values of the *b* cell edge, consistent with previous observations by Matsui and Syono (1968). The preferential stabilization of Ni in M1 arises primarily from repulsive and dispersive interactions and secondarily from the contribution of crystal-field stabilization. Excess entropy-of-mixing terms arising from ordering on sites are counterbalanced by negative heat-of-mixing terms. The mixture is thus not far from ideal in terms of Gibbs free energy over a wide range of temperatures, in agreement with the experimental observations of Campbell and Roeder (1968) and more recent findings (Seifert and O'Neill, 1987).

Introduction

Ni-Mg orthosilicates crystallize in the orthorhombic system (space group *Pbnm*). Existing structural information indicates substantial deviations from Vegard's law (Matsui and Syono, 1968) and ordering of the octahedral-site population (Bish, 1981; Rajamani et al., 1975; Boström, 1987). The present study aims at defining the structural properties of Ni-Mg olivines by X-ray refinement of the crystalline compounds after annealing at various *T* conditions. The intracrystalline disorder in the investigated solids is interpreted in terms of a Born parametrization of the cohesive energy of the crystals.

Experimental method

The crystals described in this paper were kindly supplied by Dr. Boström of Umeå University (Sweden) who performed an accurate crystallographic study of seven compositions with Ni contents of 0.0, 0.60, 0.72, 1.02, 1.38, 1.50, and 2.00 atoms per formula unit in the $Mg_{2-x}Ni_xSiO_4$ system (Boström, 1987). They were grown from a Li_2MoO_4 flux at temperatures between 890 and 1003 °C, with Li_2CO_3, SiO_2, NiO, MgO, and MoO_2 as starting materials. Crystal growth was interrupted by quenching in ice immediately after removal from the furnace (Boström, 1987).

Crystal grains were euhedral, transparent, and pale emerald in color, with mean dimensions below 0.3 mm. Table 1 shows the chemical compositions of the specimens investigated in this work, as measured by an energy-dispersive EEDS EGG spectrometer connected to a SEM AUTOSCAN electron microscope operated at 15 kV. Analyses are considered accurate to within 2–3% for major elements and to about 10% for minor ones. The standards used were pure Ni and Fe and a synthetic diopside.

All crystals contained small but significant amounts of Fe (up to 0.2% FeO); they were chemically homogeneous within analytical error and inclusion-free; optical examination showed no evidence of zoning or other imperfections. Data collection for X-ray structure refinement was performed with a STOE AED-2 four-circle diffractometer with Mo$K\alpha$ radiation monochromatized by a flat graphite crystal.

Thirty-six reflections in the range $24 < 2\theta < 41$ were accurately centered on both sides of the direct beam, to give accurate measurements of the cell parameters. Several tests repeated after changing the mounting of the crystals indicate that the σ values attached to the cell parameters in Table 2 are realistic. Intensities were measured up to $2\theta = 70°$. Refinements were performed with the STRUCSY program, distributed by STOE. Scattering curves for fully ionized atoms were used, and all structural sites were considered fully occupied. Chemical compositions of the crystals were not constrained by the results of the microprobe analyses. The refined compositions obtained from the site-occupancy refinement agreed well with the microprobe analysis for crystals Ni.30A, Ni.30B (see below), and Ni.51, but there was some discrepancy for crystals richer in Ni. The results obtained from the crystals before thermal treatment are summarized in Tables 2 and 3.

The crystals were subsequently used to achieve different states of order by heating in sealed quartz capillaries at different temperatures. The capillaries were filled with Ar fluxed on molecular sieves and Ti sponges at 800 °C. The capillary was suspended through a Pt wire in a vertical furnace and quenched in cold water at the end of the run. The time required for a temperature drop from 1200 to 500 °C was about 0.5 s. Results are summarized in Tables 2 and 3. Two Ni.30 crystals, hereafter called

0003–004X/89/0304–0411$02.00

Table 1. Chemical compositions of examined Mg–Ni olivine crystals

	Ni.30A	Ni.30B	Ni.51	Ni.68	Ni.75
MgO	34.95	34.93	22.16	13.61	10.59
NiO	27.76	27.76	43.50	54.25	58.01
FeO	0.09	0.05	0.24	0.11	0.11
SiO_2	37.21	37.27	34.10	32.01	31.27
Mg	1.400	1.397	0.969	0.634	0.505
Ni	0.600	0.599	1.026	1.363	1.492
Fe^{2+}	0.002	0.001	0.006	0.003	0.003
Si	1.000	1.000	1.000	1.000	1.000
Total	3.002	2.997	3.001	3.000	3.000

Ni.30A and Ni.30B, respectively, were used, since one was lost after the first run at 800 °C.

Quenching of the crystals by Boström (1987) was not sufficiently fast to preserve the cation distribution achieved at the synthesis temperatures (see Table 2), probably because of the large thermal mass of the material contained in the crucibles (about 20 g). In fact, our 800 °C run of Ni.30B composition led to a strong decrease in the distribution coefficient K_d ($K_d = [Mg_{M2}][Ni_{M1}]/[Mg_{M1}][Ni_{M2}]$) suggesting that the ordering of the crystal before this run occurred at temperatures lower than 800 °C, in spite of the fact that it was synthesized at 902 °C.

Structural features

Refined cell edges and volumes of untreated crystals are shown in Figure 1 and compare favorably with previous cell-edge refinement studies on synthetic binary Ni-Mg olivines (Matsui and Syono, 1968; Rajamani et al., 1975; Bish, 1981; Boström, 1987). However, we noted that annealing crystals at 800, 1150, and 1300 °C produced conspicuous variations in the *b* cell edge (*a* and *c* edges were practically unaffected) and in Ni partitioning. The variations with temperature were greatest in crystals with the Ni.30 composition (Fig. 1). In spite of the decrease in *b* with increasing temperature, no significant

Table 2. Crystal data, atomic fractional coordinates, isotropic temperature factors (B_{eq} in Å², Hamilton 1959), and occupancy factors

		Ni.30B (0.23 × 0.15 × 0.19 mm)					Ni.30A (0.23 × 0.19 × 0.06 mm)	
		902 °C			1300 °C, 1 h			
		(u)	DLS*	1150 °C, 1 h		DLS*	902 °C (u)	800 °C, 20 h
a		4.7458(5)	4.7473	4.7453(4)	4.7452(4)	4.7477	4.7466(5)	4.7459(5)
b		10.1986(6)	10.1968	10.1926(6)	10.1909(5)	10.1919	10.2003(6)	10.1950(4)
c		5.9563(6)	5.9563	5.9559(5)	5.9583(5)	5.9584	5.9556(7)	5.9559(5)
V		288.35		288.07	288.19		288.35	288.17
R eq. refl.**		0.03		0.04	0.03		0.06	0.06
R		0.022		0.035	0.021		0.032	0.039
Extinct.†		3.72×10^{-5}		9.43×10^{-5}	5.19×10^{-5}		3.51×10^{-5}	1.24×10^{-4}
K		15.6		7.1	5.7		16.9	10.6
M(1)	*x*	0.0	0.0	0.0	0.0	0.0	0.0	0.0
	y	0.0	0.0	0.0	0.0	0.0	0.0	0.0
	z	0.0	0.0	0.0	0.0	0.0	0.0	0.0
	B_{eq}	0.57		0.50	0.61		0.60	0.65
	occ. Ni	0.532(4)	0.532	0.495(7)	0.478(5)	0.478	0.533(6)	0.508(7)
M(2)	*x*	0.9900(2)	0.9902	0.9908(3)	0.9909(2)	0.9904	0.9904(3)	0.9906(3)
	y	0.2761(1)	0.2760	0.2760(1)	0.2760(1)	0.2760	0.2762(1)	0.2760(1)
	z	0.2500	0.2500	0.2500	0.2500	0.2500	0.2500	0.2500
	B_{eq}	0.62		0.56	0.67		0.64	0.70
	occ. Ni	0.068(4)	0.068	0.121(7)	0.139(4)	0.139	0.065(6)	0.089(6)
Si	*x*	0.4257(1)	0.4258	0.4257(3)	0.4262(2)	0.4260	0.4258(2)	0.4261(3)
	y	0.0936(1)	0.0936	0.0936(1)	0.0936(1)	0.0937	0.0936(1)	0.0936(1)
	z	0.2500	0.2500	0.2500	0.2500	0.2500	0.2500	0.2500
	B_{eq}	0.51		0.43	0.54		0.53	0.59
O(1)	*x*	0.7660(4)	0.7665	0.7673(7)	0.7666(4)	0.7666	0.7669(6)	0.7667(7)
	y	0.0924(2)	0.0926	0.0924(3)	0.0924(2)	0.0924	0.0925(3)	0.0927(3)
	z	0.2500	0.2500	0.2500	0.2500	0.2500	0.2500	0.2500
	B_{eq}	0.59		0.55	0.56		0.62	0.66
O(2)	*x*	0.2202(4)	0.2202	0.2198(7)	0.2199(4)	0.2201	0.2196(6)	0.2210(7)
	y	0.4461(2)	0.4460	0.4463(3)	0.4463(2)	0.4461	0.4464(3)	0.4462(3)
	z	0.2500	0.2500	0.2500	0.2500	0.2500	0.2500	0.2500
	B_{eq}	0.58		0.53	0.59		0.63	0.71
O(3)	*x*	0.2763(3)	0.2764	0.2767(5)	0.2765(3)	0.2764	0.2765(4)	0.2760(5)
	y	0.1626(1)	0.1627	0.1628(2)	0.1627(1)	0.1628	0.1626(2)	0.1628(2)
	z	0.0326(2)	0.0322	0.0324(4)	0.0322(2)	0.0324	0.0323(3)	0.0321(4)
	B_{eq}	0.62		0.56	0.65		0.66	0.73

Note: Numbers under specimen composition are the preparation temperatures (Boström, 1987); (u) means "untreated" (see text).

* Computed by DLS76.

** *R* eq. refl. = $\{\Sigma[(I_i/\sigma_i)^2 - (I_M/\sigma_i)^2]/(I_i/\sigma_i)^2\}^{1/2}$, where I_M is a weighted average between the intensities of the equivalent reflections.

† Extinct. = secondary extinction coefficient (Zachariasen, 1963).

correlation was found among changes in cation distribution, interionic distances, and angles, whose single variations are evidently masked by experimental error, whereas their added effect is evident on *b*. This result is consistent with the small differences of the crystal radii for Mg^{2+} and Ni^{2+} (0.72 and 0.69 Å respectively, according to Shannon, 1976) and the relatively small amounts of Ni displaced from M1 to M2 (always less than 0.10 atoms per formula unit). On the other hand, the disordering obtained through heating seems to lead to a slightly more regular M2 octahedron, according to the variations of the octahedral angle variance and octahedral quadratic elongation (Robinson et al., 1971).

In summary, the refined cell edges confirm substantial deviation from Vegard's law, already envisaged by Matsui and Syono (1968). Maximum thermal readjustment was observed on the *b* cell edge in the compositional range where deviation from Vegard's law reaches maximum values.

Nature of octahedral disorder

The M1 and M2 site populations determined experimentally for crystals annealed at various temperatures are conveniently interpreted by parametrization of the structure-energy properties. The method is outlined in detail in Ottonello (1987); we refer to that paper for an extensive discussion. As shown by Ottonello (1987), all interatomic distances in *Pbnm* orthosilicates except Si–O3 and O3–O3** depend on cationic radii and the M1 and M2 site occupancies, as already observed by Lumpkin and Ribbe (1983) for cell edges. Interatomic distances may then be predicted for Ni-Mg olivines with different states of intracrystalline disorder by adopting the regressions proposed by Ottonello (1987). More precise values of interatomic distances are predicted by equations of the type

$$D_n = \sum_l \sum_i \omega_{n,l,i} X_{l,i} + C_n, \qquad (1)$$

Table 2.—*Continued*

Ni.51 (0.17 × 0.15 × 0.05 mm)			Ni.68 (0.19 × 0.11 × 0.07 mm)			Ni.75 (0.28 × 0.09 × 0.06 mm)	
890 °C (u)	1150 °C	1300 °C	900 °C (u)	800 °C, 7 h	1150 °C	910 °C (u)	1150 °C
4.7392(4)	4.7431(7)	4.7398(9)	4.7393(5)	4.7345(5)	4.7370(6)	4.7339(8)	4.7350(9)
10.1939(6)	10.1765(8)	10.1773(11)	10.1620(6)	10.1623(6)	10.1616(6)	10.1583(8)	10.1526(9)
5.9432(6)	5.9401(9)	5.9443(11)	5.9330(6)	5.9317(6)	5.9337(6)	5.9303(8)	5.9278(8)
287.12	286.72	286.74	285.74	285.39	285.62	285.18	284.96
0.04	0.06	0.04	0.12	0.08	0.05	0.08	0.10
0.028	0.036	0.027	0.065	0.041	0.030	0.029	0.044
1.51×10^{-5}	7.10×10^{-5}	1.10×10^{-5}	1.71×10^{-5}	1.40×10^{-4}	5.07×10^{-5}	5.74×10^{-5}	7.25×10^{-5}
11.4	5.3	5.7	7.4	7.5	5.5	12.0	4.8
0.0	0.0	0.0	0.0	0.0	0.0	0.0	0.0
0.0	0.0	0.0	0.0	0.0	0.0	0.0	0.0
0.0	0.0	0.0	0.0	0.0	0.0	0.0	0.0
0.51	0.51	0.64	0.54	0.34	0.54	0.55	0.43
0.788(9)	0.710(9)	0.705(8)	0.87(2)	0.88(2)	0.864(9)	0.95(1)	0.87(2)
0.9901(3)	0.9913(3)	0.9911(3)	0.9912(5)	0.9917(4)	0.9916(2)	0.9919(2)	0.9918(3)
0.2751(1)	0.2751(1)	0.2752(1)	0.2748(2)	0.2744(1)	0.2744(1)	0.2742(1)	0.2745(1)
0.2500	0.2500	0.2500	0.2500	0.2500	0.2500	0.2500	0.2500
0.59	0.52	0.67	0.57	0.39	0.56	0.60	0.45
0.246(7)	0.320(10)	0.294(7)	0.47(2)	0.50(1)	0.535(8)	0.60(1)	0.59(1)
0.4252(3)	0.4265(4)	0.4262(3)	0.4259(6)	0.4266(5)	0.4266(3)	0.4266(4)	0.4267(5)
0.0936(1)	0.0936(2)	0.0936(1)	0.0930(3)	0.0937(2)	0.0938(1)	0.0938(2)	0.0938(3)
0.2500	0.2500	0.2500	0.2500	0.2500	0.2500	0.2500	0.2500
0.47	0.47	0.57	0.51	0.35	0.50	0.52	0.46
0.7670(8)	0.7685(10)	0.7669(9)	0.7692(18)	0.7677(13)	0.7679(7)	0.7669(9)	0.7684(13)
0.0929(3)	0.0929(5)	0.0926(3)	0.0930(7)	0.0936(6)	0.931(3)	0.0932(4)	0.0929(6)
0.2500	0.2500	0.2500	0.2500	0.2500	0.2500	0.2500	0.2500
0.59	0.51	0.74	0.62	0.37	0.59	0.58	0.47
0.2186(8)	0.2200(10)	0.2194(8)	0.2174(17)	0.2194(14)	0.2178(7)	0.2189(9)	0.2198(14)
0.4455(4)	0.4462(5)	0.4462(3)	0.4454(8)	0.4455(6)	0.4454(3)	0.4451(4)	0.4449(6)
0.2500	0.2500	0.2500	0.2500	0.2500	0.2500	0.2500	0.2500
0.54	0.56	0.66	0.60	0.41	0.57	0.61	0.57
0.2762(4)	0.2745(7)	0.2765(6)	0.2760(12)	0.2735(9)	0.2745(5)	0.2744(6)	0.2750(9)
0.1627(2)	0.1626(3)	0.1622(2)	0.1629(5)	0.1626(4)	0.1626(2)	0.1627(3)	0.1630(4)
0.0324(4)	0.0326(6)	0.0320(4)	0.0319(10)	0.0314(8)	0.0312(4)	0.0315(5)	0.0319(8)
0.59	0.63	0.70	0.73	0.41	0.62	0.58	0.52

TABLE 3. Interatomic distances, volumes, octahedral and tetrahedral quadratic elongation (OQE, TQE), octahedral and tetrahedral angular variance (OAV, TAV), according to Robinson et al. (1971)

	Ni.30B			Ni.30A		Ni.51		
	902 °C (u)	1150 °C, 1h	1300 °C, 1 h	902 °C (u)	800 °C	890 °C (u)	1150 °C, 1 h	1300 °C, 1 h
M1–O1 ×2	2.083(1)	2.079(2)	2.082(1)	2.081(2)	2.082(2)	2.079(2)	2.075(3)	2.078(2)
M1–O2 ×2	2.070(1)	2.070(2)	2.070(1)	2.071(2)	2.067(2)	2.072(2)	2.066(3)	2.068(2)
M1–O3 ×2	2.123(1)	2.125(2)	2.123(1)	2.124(2)	2.123(2)	2.121(2)	2.114(3)	2.116(2)
⟨M1–O⟩	2.092(3)	2.091(5)	2.092(3)	2.092(5)	2.091(5)	2.091(6)	2.085(8)	2.087(6)
Volume	11.75(1)	11.74(2)	11.74(1)	11.74(2)	11.73(2)	11.73(2)	11.63(2)	11.67(2)
OQE(M1)	1.0259	1.0263	1.0261	1.0262	1.0257	1.0257	1.0262	1.0262
OAV(M1)	92.05	93.20	92.59	93.07	91.34	91.19	93.46	92.95
M2–O1	2.154(2)	2.151(3)	2.153(2)	2.153(3)	2.149(3)	2.136(4)	2.134(5)	2.140(4)
M2–O2	2.049(2)	2.047(3)	2.048(2)	2.049(3)	2.051(3)	2.046(4)	2.052(5)	2.050(4)
M2–O3 ×2	2.062(1)	2.062(2)	2.062(2)	2.061(2)	2.061(3)	2.061(3)	2.068(3)	2.062(3)
M2–O3′ ×2	2.206(1)	2.202(2)	2.203(1)	2.206(2)	2.202(2)	2.195(3)	2.187(4)	2.198(3)
⟨M2–O⟩	2.123(4)	2.121(7)	2.122(4)	2.123(6)	2.121(7)	2.116(7)	2.116(11)	2.118(7)
Volume	12.32(1)	12.28(1)	12.35(1)	12.31(1)	12.29(2)	12.20(2)	12.21(2)	12.25(2)
OQE(M2)	1.0251	1.0249	1.0244	1.0251	1.0244	1.0241	1.0235	1.0240
OAV(M2)	86.41	85.83	84.06	86.44	84.09	83.34	81.93	83.09
Si–O1	1.615(2)	1.621(3)	1.616(2)	1.619(3)	1.616(3)	1.620(4)	1.622(5)	1.615(4)
Si–O2	1.656(2)	1.653(3)	1.654(2)	1.653(3)	1.657(3)	1.655(4)	16.53(5)	1.652(4)
Si–O3 ×2	1.636(1)	1.636(2)	1.639(2)	1.637(2)	1.640(2)	1.633(3)	1.637(4)	1.634(3)
⟨Si–O⟩	1.636(3)	1.636(6)	1.637(3)	1.636(5)	1.638(6)	1.635(6)	1.638(8)	1.633(3)
Volume	2.210(2)	2.214(4)	2.214(2)	2.213(3)	2.220(4)	2.210(4)	2.213(6)	2.201(4)
TQE	1.0107	1.0105	1.0118	1.0107	1.0110	1.0101	1.0121	1.0109
TAV	47.52	46.17	47.98	43.04	49.07	44.43	53.13	48.25

$$\mathrm{OAV} = \sum_{i=1}^{12} (A_i - 90)^2/11,$$

where A_i values are the angles O–M–O.

$$\mathrm{TAV} = \sum_{i=1}^{6} (A_i - 109.47)^2/5,$$

where A_i values are the tetrahedral angles O–T–O.

$$\mathrm{OQE} = \sum_{i=1}^{6} (l_i/l_0)^2/6,$$

where l_0 is the center-to-vertex distance for a regular octahedron whose volume is equal to that of a real octahedron with bond lengths l_i.

$$\mathrm{TQE} = \sum_{i=1}^{4} (l_i/l_0)^2/4,$$

where l_0 is the center-to-vertex distance for a regular tetrahedron whose volume is equal to that of a real tetrahedron with bond lengths l_i.

where n refers to the coefficients listed in Table 4, C_n is a constant, $X_{l,i}$ is the occupancy of ion i on site l, and $\omega_{n,l,i}$ are ionic factors. The latter are not simply represented by ionic radii in sixfold coordination (as in Lumpkin and Ribbe, 1983, and Ottonello, 1987), but are linearly dependent on ionic potentials and polarizability of the various ionic species (work in progress). The values of ω and C that satisfy the observed interatomic distances in Ni-Mg olivines are shown in Table 4.

The calculated distances were then further refined by a "least-squares-distance" method (DLS-76 computer program by Baerlocher et al., 1977), resulting in an optimized structure that reproduces the actual crystal with high precision. As an example, compare the experimental data in Table 2 (columns 1 and 3) with the calculated values (columns 4 and 5) for the Ni.30B crystal. The calculated values also clearly reproduce the increase in b with ordering ($\Delta b_{obs} = 0.008$ Å, $\Delta b_{calc} = 0.007$ Å).

The fractional coordinates of the various atoms (M1, M2, Si, O1, O2, O3) in the asymmetric unit, as determined in this way, were used to perform lattice-energy calculation by Ewald's method following the equations (Catti, 1981)

$$U_L = E_C + E_R + E_D \quad (2)$$

$$E_C = \sum_{i=1}^{n} \sum_{j=i}^{n} Z_i Z_j C_{ij}^{el} \quad (3)$$

$$E_R = \sum_{i=1}^{n} \sum_{j=i}^{n} b_{ij} C_{ij}^{R} \quad (4)$$

TABLE 3.—*Continued*

Ni.68			Ni.75	
900 °C (u)	800 °C, 7 h	1300 °C, 1 h	910 °C (u)	1150 °C, 1 h
2.071(5)	2.077(4)	2.075(2)	2.077(3)	2.071(4)
2.074(5)	2.067(4)	2.073(2)	2.069(3)	2.066(4)
2.118(5)	2.108(4)	2.111(2)	2.110(3)	2.114(4)
2.088(13)	2.084(11)	2.086(5)	2.085(7)	2.084(11)
11.68(4)	11.63(3)	11.66(2)	11.66(2)	11.63(3)
1.0259	1.0250	1.0252	1.0248	1.0249
91.98	89.13	89.70	88.22	88.57
2.126(8)	2.121(7)	2.125(3)	2.125(4)	2.125(7)
2.038(8)	2.046(7)	2.041(3)	2.041(5)	2.040(6)
2.059(6)	2.064(4)	2.062(2)	2.063(3)	2.061(4)
2.189(6)	2.180(6)	2.184(2)	2.180(3)	2.179(4)
2.110(17)	2.109(13)	2.110(7)	2.109(9)	2.108(13)
12.11(4)	12.12(4)	12.13(2)	12.11(3)	12.09(3)
1.0235	1.0220	1.0224	1.0221	1.0225
81.16	76.92	77.87	76.97	78.25
1.627(9)	1.615(7)	1.617(3)	1.611(5)	1.618(7)
1.647(8)	1.657(7)	1.656(3)	1.660(5)	1.662(7)
1.638(6)	1.643(5)	1.641(2)	1.639(3)	1.638(5)
1.637(14)	1.639(11)	1.639(6)	1.638(7)	1.639(11)
2.219(9)	2.222(7)	2.221(4)	2.216(5)	2.222(7)
1.0104	1.0117	1.0112	1.0113	1.0114
45.23	52.48	49.81	50.66	50.67

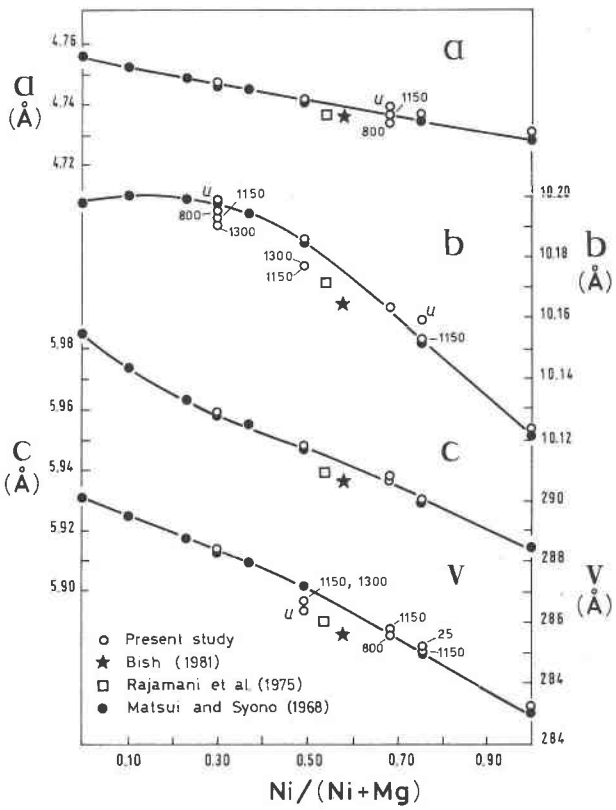

Fig. 1. Composition dependence of unit-cell parameters and volume in $(Ni,Mg)_2SiO_4$ olivine mixtures. The (u) (= untreated) refers to sample before thermal runs. A single open circle means that data for sample before and after thermal treatment overlap.

$$E_D = E_{DD} + E_{DQ} = \sum_{i=1}^{n}\sum_{j=i}^{n} dd_{ij}C_{ij}^{dd} + \sum_{i=1}^{n}\sum_{j=1}^{n} dq_{ij}C_{ij}^{dq}, \quad (5)$$

where Z_i, Z_j are formal ionic charges for i, j ions.

In the above equations, the lattice energy (U_L) of Ni-Mg olivines is considered to be composed of Coulombic (E_C), repulsive (E_R), and dispersive (E_{DD}, E_{DQ}) contributions; charge (C_{ij}^{el}), repulsive (C_{ij}^{R}), and dispersive coefficients (C_{ij}^{dd}, C_{ij}^{dq}) were generated by Ewald's summation. Repulsive and dispersive parameters (b_{ij}, dd_{ij}, dq_{ij}) derived from the Born theory for ionic solids (Tosi, 1964; Ottonello, 1987) are shown in Table 5.

Energy contributions arising from crystal-field stabilization of Ni^{2+} ions in the M1 and M2 octahedra may possibly be reproduced by a linear expression based on site occupancy as follows:

$$E_{CFSE} = -114.22x_{Ni,M1} - 107.53x_{Ni,M2}, \quad (6)$$

where energy is in kJ/mol. The energy terms pertinent to each site are those derived by Wood (1974) for a synthetic mixture of composition $(Mg_{0.9}Ni_{0.1})_2SiO_4$ and are here assumed to be valid over the whole binary range. The values of the enthalpy of formation from the elements at standard state (H_f^0) are easily derived by applying the Born-Haber-Fayans thermochemical cycle to the obtained U_L values (cf. Eq. 2 in Ottonello, 1987). Enthalpy at the considered temperature and 1 bar is then computed by the thermodynamic relation

$$H_{T,P_r} = H^0_{f,T_r,P_r} + \int_{T_r}^{T} C_p\, dT. \quad (7)$$

Isobaric heat capacity (C_P) is a polynomial function in T. It is easily calculated from tabulated values for end-members and constituent oxides (Helgeson et al., 1978), as C_P is not appreciably dependent on the state of intracrystalline disorder (cf. Berman and Brown, 1985). The

TABLE 4. Coefficients to be applied to each ion fraction on each site to obtain the interatomic distances through Equation 1

	$\omega_{Mg,M1}$	$\omega_{Ni,M1}$	$\omega_{Mg,M2}$	$\omega_{Ni,M2}$	C
T–O1A	1.2142	1.2191	0.0710	0.0699	0.3299
T–O2A	1.2612	1.2579	0.0646	0.0652	0.3327
T–O3A	1.2387	1.2365	0.0699	0.0596	0.3310
Mean T–O	1.2227	1.2221	0.0977	0.0924	0.3177
O1A–O2A	2.3082	2.3144	0.1058	0.0864	0.3359
O1A–O3A	1.0326	1.0276	−0.9766	−0.9702	2.7041
O2A–O3A	2.1914	2.1950	0.1275	0.1163	0.2417
O3A–O3B	2.1615	2.1543	0.1188	0.0925	0.3196
M1–O1B	0.3817	0.3745	−0.4564	−0.4715	2.1621
M1–O2A	1.2498	1.2468	0.5103	0.5173	0.3108
M1–O3A	1.3873	1.3751	0.3520	0.3412	0.3913
Mean M1–O	0.5687	0.5605	−0.6536	−0.6593	2.1817
O1B–O2A	2.3570	2.3703	0.1679	0.1642	0.3269
O1B–O3A	2.3510	2.3214	0.1758	0.1550	0.3281
O1B–O3C	2,7201	2.7109	0.1458	0.1344	0.2450
O2A–O3C	3.0326	3.0021	−0.0215	−0.0133	0.3250
O1B–O2B	2.5773	2.5498	0.1272	0.1200	0.3227
M2–O1A	1.3204	1.2757	0.5087	0.4908	0.3467
M2–O2C	−0.1773	−0.1800	0.9425	0.9242	1.2864
M2–O3D	1.3131	1.2939	0.5437	0.5067	0.3614
M2–O3E	1.3037	1.2948	0.4365	0.4482	0.3246
Mean M2–O	1.3057	1.2890	0.4832	0.4683	0.3433
O1A–O3E	2.5614	2.5373	0.1041	0.0902	0.3576
O3D–O3F	0.1257	0.1249	0.7912	0.7725	2.0771
O3E–O3F	2.9630	2.9120	0.0813	0.0916	0.3442
O2C–O3D	2.6171	2.6053	0.1959	0.1627	0.3739
O2C–O3E	2.5937	2.5607	0.0128	0.0037	0.3260
a	3.8262	3.8044	0.6010	0.5935	0.3323
b	3.4996	3.4842	5.0357	4.9631	1.6749
c	3.8600	3.8003	1.7180	1.7027	0.4112
V	280.027	275.985	−118.127	−121.683	128.798

	x	y	z		Symmetry operations		
T	0.45	0.09	0.25				
M1	0.00	0.00	0.00				
M2	0.99	0.28	0.25				
O1A	0.77	0.09	0.25	O1B	$-1 + X$	Y	Z
O2A	0.24	−0.05	0.25	O2B	$-X$	$-Y$	$-Z$
				O2C	$3/2 - X$	$1/2 + Y$	Z
O3A	0.28	0.16	0.03	O3B	X	Y	$1/2 - Z$
				O3C	$-X$	$-Y$	$-Z$
				O3D	$1 + X$	Y	Z
				O3E	$1/2 + X$	$1/2 - Y$	$1/2 + Z$
				O3F	$1/2 + X$	$1/2 - Y$	$-Z$

Gibbs free energy at the considered T and 1 bar is calculated by applying

$$G_{T,P_r} = H^0_{f,T_r,P_r} - T\left(S^0_{T_r,P_r} + \int_{T_r}^{T} C_P\, dT/T\right) \quad (8)$$

in which $S^0_{T_r,P_r}$ is the entropy of the compound at standard state. The standard entropy may be calculated from tabulated values for isostructural solids and constituent oxides by applying the corrective factors based on molar volumes (cf. Helgeson et al., 1978) and adding a configurational term (S^0_{mix}), because of the disordering on M1 and M2 octahedral positions, expressed in the form

$$S^0_{mix} = -R\left(\sum_i X_{i,M1} \ln X_{i,M1} + \sum_i X_{i,M2} \ln X_{i,M2}\right) \quad (9)$$

Calculated values of E_C, E_R, E_{DD}, E_{DQ}, E_{CFSE}, U_L, H^0, G^0, S^0 obtained with a hardness factor $\rho = 0.20$ are shown in Table 6. For comparative purposes, calculations were performed on seven binary compositions with variable Ni/(Ni + Mg) (plus two end-members), and five different conditions of octahedral disorder were evaluated for each particular composition. It is immediately clear from Table 6 that, based on the principle of minimization of Gibbs free energy at equilibrium (Zemansky, 1957), the stable configuration at standard state is achieved for all compositions when all the Ni is in M1 sites. A close look at the lattice-energy constituents reveals that this is primarily due to repulsive (E_R) and dispersive (E_{DD}, E_{DQ}) contributions, whereas the Coulombic term tends to stabilize Ni in M2 sites. Accounting for energy contributions arising from crystal-field stabilization of Ni^{2+} ion on M1 and M2 sites (case 2 in Table 6) or disregarding it (case 1 in Table 6) has a limited influence in the calculation, CFSE being subordinate to even dipole-quadrupole interactions in terms of energy. Accounting for CFSE may lead to

TABLE 5. Coefficients of repulsive and dispersive energy

Ion	Ion	$b_{ij} \times 10^{19}$ (1)	$b_{ij} \times 10^{19}$ (2)	$b_{ij} \times 10^{19}$ (3)	dd_{ij} ($\times 10^{19}$ J·Å^6)	dq_{ij} ($\times 10^{19}$ J·Å^8)
Ni	Ni	3 549.095	3 744.732	2 715.474	19.371	31.795
Ni	Si	477.207	497.036	399.290	1.053	1.021
Ni	O	81 497.937	84 884.312	51 981.516	36.025	73.386
Mg	Mg	4 588.848	4 588.848	3 280.789	0.336	0.165
Mg	Si	542.625	550.211	438.889	0.169	0.067
Mg	O	92 669.875	93 965.375	57 136.625	4.173	6.101
Ni	Mg	4 035.635	4 145.367	2 984.783	2.371	2.528
Si	Si	62.855	64.625	57.514	0.098	0.029
Si	O	10 623.484	10 922.586	7 445.449	1.782	2.434
O	O	1 403 580.505	1 443 104.093	746 299.750	68.613	166.928

Note: Coefficients of repulsive (b_{ij}), and dispersive (dipole-dipole = dd_{ij} and dipole-quadrupole = dq_{ij}) energy. Values of b_{ij} are relative to $\rho = 0.20$ without CFSE (1), to $\rho = 0.20$ with CFSE (2), and to $\rho = 0.21$ with CFSE (3).

further stabilization of Ni^{2+} ions in M1 (see also Table 6).

The energy term arising from configurational disorder ($-TS^{0}_{mix}$; cf. Eqs. 8, 9) obviously plays an increasing role with increasing temperature (T), and minimum Gibbs free-energy states at high T show partial disorder between M1 and M2 sites. Precise values for the equilibrium degree of internal disorder at different temperatures and compositions are obtained by an appropriate mathematical treatment of the tabulated data, as outlined in Ottonello (1987). Table 7 shows the results of calculations, in terms of K_d, for two different values of the hardness factor ($\rho = 0.20$ and 0.21, respectively) and in the presence and absence of CFSE ($\rho = 0.20$). It may be seen that, in terms of intracrystalline disorder, accounting for CFSE has the same effect as that obtained by lowering the hardness factor ρ; however, as will be shown, accounting for CFSE results in a more precise evaluation of energy properties of the mixture. Figure 2 compares the intracrystalline disorder given by structure-energy calculations with the experimental results. As already noted, theoretical calculations predict substantial ordering of Ni in M1 and increased disorder with increasing T, in agreement with experimental evidence. Agreement is satisfactory at T = 1300 °C, the computed K_d field being near (and partially superimposed on) Boström's (1987) and our results, whereas the untreated samples are more ordered with respect to theoretical predictions. However, the scatter of points for Mg-rich untreated compositions leaves little doubt that the quenching procedure used by Boström (1987) was not rapid enough to avoid partial reordering, as already discussed. Small anomalous increases in K_d with T observed experimentally in some heat-treated samples (Ni.51 at 1300 °C) are most probably ascribable to uncertainties in site-occupancy determinations, which are worst for Ni-rich compositions.

Nature of solid mixtures investigated

Figure 3 shows values of excess Gibbs free energy of mixing (G^{exc}_{mix}), excess enthalpy, (H^{exc}_{mix}) and excess entropy ($-TS^{exc}_{mix}$), generated by structure-energy calculations with $\rho = 0.21$ in the presence of CFSE. (These excess properties are defined relative to an ideal solid mixture.) Excess Gibbs free energy is very limited over a wide temperature range (600 °C < T < 1400 °C) and markedly negative at stan-

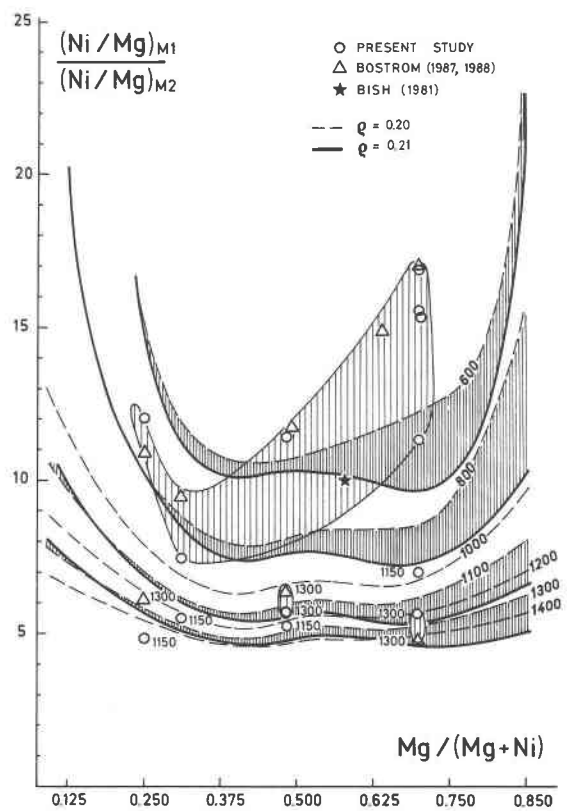

Fig. 2. Observed and calculated intracrystalline disorder vs. composition. Dashed lines show K_d calculated with $\rho = 0.20$ for 600 °C < T < 1400 °C. Results with $\rho = 0.21$ (Table 7) are shown by heavy lines for T = 600, 800, 1100, and 1300 °C. Shaded areas encompass K_d values calculated with identical T conditions, but different hardness factors. Symbols without temperature label (large light-shaded area) are K_d values of untreated specimens.

TABLE 6. Constituents of bulk lattice energy for Ni-Mg olivines with various stages of intracrystalline (M1-M2) disorder

Ni/(Ni + Mg)	$X_{Ni,M1}$	$X_{Ni,M2}$	E_C	E_R (1)	E_{DD}	E_{DQ}	E_{CFSE}	U_L (1)	$H^0_{T,P(r)}$ (1)	S^0_{mix}	$S^0_{T(r),P(r)}$
1.000	1.0000	1.0000	−24232.590	4023.092	−585.667	−219.941	−221.750	−21015.098	−1405.227	0.000	110.039
0.875	1.0000	0.7500	−24206.270	3982.530	−542.861	−201.174	−194.868	−20967.773	−1502.078	4.676	112.859
0.875	0.9375	0.8125	−24212.055	3989.506	−542.493	−200.979	−194.449	−20966.418	−1500.324	5.956	114.140
0.875	0.8750	0.8750	−24217.125	3995.653	−542.044	−200.747	−194.031	−20964.266	−1498.570	6.266	114.449
0.875	0.8125	0.9375	−24222.125	4001.683	−541.561	−200.495	−193.613	−20962.500	−1496.805	5.956	114.140
0.875	0.7500	1.0000	−24227.262	4008.322	−541.098	−200.256	−193.195	−20960.293	−1494.598	4.676	112.859
0.750	1.0000	0.5000	−24180.523	3943.315	−500.868	−182.815	−167.985	−20920.891	−1599.387	5.764	112.090
0.750	0.8750	0.6250	−24191.078	3955.354	−500.060	−182.377	−167.149	−20918.160	−1596.656	8.633	114.960
0.750	0.7500	0.7500	−24200.941	3967.495	−499.193	−181.906	−166.313	−20914.547	−1593.043	9.351	115.678
0.750	0.6250	0.8750	−24212.199	3981.407	−498.237	−181.404	−165.476	−20910.434	−1588.930	8.633	114.960
0.750	0.5000	1.0000	−24221.914	3994.370	−497.181	−180.852	−164.640	−20905.578	−1584.074	5.763	112.090
0.625	1.0000	0.2500	−24154.738	3905.662	−459.715	−164.876	−141.103	−20873.668	−1696.359	4.676	109.145
0.625	0.8125	0.4375	−24170.102	3922.320	−458.513	−164.199	−139.848	−20870.492	−1693.184	9.711	114.180
0.625	0.6260	0.6250	−24185.914	3940.832	−457.159	−163.453	−138.594	−20865.703	−1688.395	11.001	115.471
0.625	0.4375	0.8125	−24201.309	3960.498	−455.631	−162.632	−137.339	−20859.074	−1681.766	9.711	114.180
0.625	0.2500	1.0000	−24216.777	3981.792	−453.954	−161.751	−136.085	−20850.691	−1673.383	4.676	109.145
0.500	1.0000	0.0000	−24129.184	3868.885	−419.260	−147.271	−114.220	−20826.828	−1793.695	0.000	102.613
0.500	0.7500	0.2500	−24150.223	3890.809	−417.786	−146.412	−112.548	−20823.609	−1790.477	9.352	111.964
0.500	0.5000	0.5000	−24170.570	3914.494	−415.942	−145.375	−110.875	−20817.395	−1774.262	11.527	114.140
0.500	0.2500	0.7500	−24190.512	3940.036	−413.762	−144.192	−109.203	−20808.430	−1775.297	9.352	111.964
0.500	0.0000	1.0000	−24211.059	3968.766	−411.291	−142.893	−107.530	−20769.477	−1763.344	0.000	102.613
0.375	0.0000	0.3750	−24185.313	3927.522	−371.977	−125.735	−82.648	−20755.500	−1866.559	4.676	105.432
0.375	0.1875	0.5625	−24170.117	3907.131	−373.811	−126.721	−81.902	−20763.520	−1874.578	9.711	110.467
0.375	0.3750	0.3750	−24155.340	3888.520	−375.476	−127.641	−83.136	−20769.934	−1880.992	11.001	111.758
0.375	0.5625	0.1875	−24139.926	3870.545	−376.937	−128.467	−84.411	−20774.785	−1885.844	9.711	110.467
0.375	0.7500	0.0000	−24124.590	3853.871	−378.193	−129.203	−85.665	−20778.113	−1889.172	4.676	105.432
0.250	0.0000	0.5000	−24159.684	3887.861	−333.429	−108.958	−53.765	−20714.211	−1969.495	5.763	104.663
0.250	0.1250	0.3750	−24150.242	3875.244	−334.639	−109.623	−54.601	−20719.258	−1974.492	8.633	107.533
0.250	0.2500	0.2500	−24139.945	3862.652	−335.740	−110.243	−55.138	−20723.277	−1978.512	9.351	108.251
0.250	0.3750	0.1250	−24130.035	3850.870	−336.769	−110.827	−56.274	−20726.762	−1981.996	8.633	107.533
0.250	0.5000	0.0000	−24119.367	3839.135	−337.691	−111.363	−57.110	−20729.285	−1984.520	5.763	104.663
0.125	0.0000	0.2500	−24134.348	3849.298	−295.599	−92.528	−26.883	−20673.176	−2072.602	4.676	101.718
0.125	0.0625	0.1875	−24129.988	3843.643	−296.194	−92.861	−27.301	−20675.398	−2074.824	5.956	102.999
0.125	0.1250	0.1250	−24124.500	3837.113	−296.737	−93.171	−27.719	−20677.293	−2076.719	6.266	103.308
0.125	0.1875	0.0625	−24119.539	3831.278	−297.281	−93.480	−28.137	−20679.023	−2078.449	5.956	102.999
0.125	0.2500	0.0000	−24114.141	3824.996	−297.772	−93.769	−28.555	−20680.688	−2080.113	4.676	101.718
0.000	0.0000	0.0000	−24109.539	3812.287	−258.450	−76.423	0.000	−20632.125	−2175.727	0.000	95.186

Note: Coulombic (E_C), repulsive (E_R), dispersive (E_{DD}, E_{DQ}), and crystal-field stabilization (E_{CFSE}) constituents of bulk lattice energy (U_L) for Ni-Mg olivines with various states of intracrystalline (M1-M2) disorder. Standard state (T = 298.15 °K, 1 bar) enthalpy $H^0_{T(r),P(r)}$, entropy $S^0_{T(r),P(r)}$, and free energy $G^0_{T(r),P(r)}$ are also listed. S^0_{mix} is the mixing entropy arising from configurational disorder in M1-M2 sites. (1) Calculated neglecting CFSE contribution to the bulk lattice energy; (2) calculated accounting for CFSE effects. All data are relative to ρ = 0.20. All figures must be kept as significant to avoid rounding errors. All energy data but S^0_{mix} and $S^0_{T(r),P(r)}$ expressed in kj·mol^{-1}. S^0_{mix} and $S^0_{T(r),P(r)}$ are in J·mol^{-1}·K^{-1}.

dard-state conditions (T = 25 °C). Excess entropy effects arising from ordering on sites (positive $-TS^{exc}_{mix}$ contribution to G^{exc}_{mix}) are in fact counterbalanced by the negative heat-of-mixing terms (H^{exc}_{mix}). Activities are in good agreement with the experimental observations of Campbell and Roeder (1968) (Table 8) at high T (1400 °C) and with recent findings by Seifert and O'Neill (1987) at lower T. Agreement is less satisfactory with respect to the results of galvanic cell emf measurements (Ottonello and Morlotti, 1987; Boström and Rosen, 1988; cf. Table 8). However, we note that the isoactivity region observed by Ottonello and Morlotti (1987) and ascribed to the presence

TABLE 7. Intracrystalline distribution factors $K_d = [Mg_{M2}][Ni_{M1}]/[Mg_{M1}][Ni_{M2}]$ in Ni-Mg olivines according to the structure-energy parametrization

	Mg = 0.125			Mg = 0.250			Mg = 0.375			Mg = 0.500			Mg = 0.625		
T (°C)	(1)	(2)	(3)	(1)	(2)	(3)	(1)	(2)	(3)	(1)	(2)	(3)	(1)	(2)	(3)
25	—	—	—	—	—	—	—	—	—	76.80	677.0	71.10	—	—	—
600	86.80	—	131	15.20	46.50	15.00	10.80	19.20	10.00	10.80	19.20	10.00	11.50	20.90	9.95
800	19.50	—	21.30	10.40	22.10	10.30	7.92	14.50	7.58	8.27	13.30	7.61	8.42	13.60	7.31
1000	11.60	51.20	12.20	7.97	14.30	8.04	6.40	10.40	6.09	6.68	10.10	6.17	6.61	9.95	5.85
1100	9.70	28.20	9.91	7.14	12.20	7.26	5.75	9.23	5.57	6.05	9.00	5.71	5.99	8.81	5.35
1200	8.35	20.20	8.60	6.48	10.60	6.59	5.35	8.27	5.07	5.55	8.27	5.19	5.53	7.92	4.95
1300	7.35	16.00	7.48	5.95	9.37	6.05	4.99	7.51	4.73	5.19	7.46	4.86	5.11	7.13	4.59
1400	6.54	13.3	6.70	5.57	8.48	5.61	4.62	6.95	4.42	4.86	6.88	4.52	4.77	6.61	4.25

Note: Calculated with (1) ρ = 0.20, neglecting CFSE contributions; (2) ρ = 0.20 with CFSE; (3) ρ = 0.21 with CFSE.

TABLE 6.—*Continued*

$G^0_{T(r),P(r)}$ (1)	E_R (2)	U_L (2)	$H^0_{T(r),P(r)}$ (2)	$G^0_{T(r),P(r)}$ (2)
−1438.035	4244.842	−21015.106	−1405.234	−1438.043
−1535.727	4174.856	−20970.313	−1504.617	−1538.266
−1534.355	4182.055	−20967.918	−1502.223	−1536.253
−1532.693	4188.383	−20965.563	−1499.871	−1533.994
−1530.835	4194.578	−20963.211	−1497.519	−1531.550
−1528.246	4201.410	−20960.395	−1494.703	−1528.351
−1632.806	4106.840	−20925.348	−1603.844	−1637.264
−1630.931	4119.156	−20921.508	−1600.004	−1634.279
−1627.532	4131.551	−20916.797	−1595.297	−1629.786
−1623.205	4145.773	−20911.539	−1590.039	−1624.314
−1617.494	4158.988	−20905.598	−1584.097	−1617.516
−1728.901	4040.996	−20879.438	−1702.130	−1734.671
−1722.226	4057.893	−20874.770	−1697.461	−1731.504
−1722.822	4076.651	−20868.465	−1691.160	−1725.587
−1715.808	4096.574	−20860.332	−1683.027	−1717.070
−1705.924	4118.129	−20850.434	−1673.128	−1705.669
−1824.289	3976.566	−20833.367	−1800.236	−1830.830
−1823.859	3998.661	−20828.305	−1795.172	−1828.554
−1818.292	4022.469	−20820.293	−1787.160	−1821.191
−1808.679	4048.107	−20809.559	−1776.429	−1809.811
−1793.938	4076.950	−20795.820	−1762.690	−1793.284
−1897.993	4007.829	−20755.840	−1866.901	−1898.336
−1907.514	3987.525	−20765.023	−1876.085	−1909.021
−1914.313	3968.998	−20772.609	−1883.672	−1916.992
−1918.779	3951.076	−20778.664	−1889.723	−1922.658
−1920.606	3934.435	−20783.215	−1894.274	−1925.709
−2000.650	3940.872	−20714.961	−1970.199	−2001.404
−2006.553	3928.420	−20720.680	−1975.918	−2007.978
−2010.787	3915.975	−20725.387	−1980.625	−2012.900
−2014.057	3904.332	−20729.574	−1984.809	−2016.870
−2015.725	3892.713	−20732.816	−1988.051	−2019.256
−2102.929	3875.552	−20673.801	−2073.230	−2103.557
−2105.533	3870.026	−20676.313	−2075.742	−2106.451
−2107.520	3863.615	−20678.512	−2077.938	−2108.739
−2109.158	3857.898	−20680.539	−2079.965	−2110.674
−2110.440	3851.727	−20682.512	−2081.938	−2112.265
−2204.106	3812.287	−20632.125	−2175.727	−2204.106

of the mixed silicate $Ni_{0.25}Mg_{0.75}Si_{0.5}O_2$ with limited solubility for $NiSi_{0.5}O_2$ cannot be reproduced by the model, which implicitly assumes *Pbnm* symmetry for all compounds in the binary field.

CONCLUSIONS

The present study shows that, in Ni-Mg olivines, Ni is preferentially stabilized in the M1 site at all investigated T conditions. Moreover, structure refinements show conspicuous deviations from Vegard's law, as also observed in previous studies (Matsui and Syono, 1968; Rajamani et al., 1975; Bish, 1981; Boström, 1987). The Born parametrization of the cohesive energy of the crystals confirms that, at standard state (T = 298.15 K, P = 1 bar), the minimum Gibbs free energy of the system is attained when all the Ni is in M1. The incipient disorder observed at high T is primarily due to the energy term $-TS$, while enthalpic contributions would favor full ordering of Ni in M1 at all T conditions. The preferential stabilization of Ni in M1, in terms of heat content, arises from the repulsive and dispersive constituents of lattice energy, the role of CFSE being very subordinate. The Gibbs free energy properties shown by the model are not far from an ideal mixture in a wide T-range, although they are slightly asymmetric (cf. Fig. 3).

TABLE 7.—*Continued*

Mg = 0.750			Mg = 0.875		
(1)	(2)	(3)	(1)	(2)	(3)
—	—	—	—	—	—
12.70	21.70	10.30	53.50	—	34.00
9.20	13.80	7.70	15.70	42.40	10.10
7.26	10.30	6.28	9.60	16.00	7.10
6.54	8.95	5.73	8.05	12.30	6.23
6.00	8.18	5.25	7.04	10.30	5.68
5.52	7.32	4.85	6.23	8.68	5.09
5.17	6.74	4.59	5.68	6.69	4.75

TABLE 8. Comparison between model-predicted activities and experimental observations

T = 1400 °C				T = 1000 °C				
$X_{Ni_2SiO_4}$	(1)	(2)	(3)	$X_{Ni_2SiO_4}$	(1)	(2)	(4)	(5)
0.18	0.13	0.19	0.18	0.18	0.24	0.18	0.15	—
0.22	0.31	0.25	0.26	0.21	0.30	0.23	—	0.55
0.35	0.43	0.37	0.39	0.33	0.43	0.36	0.28	—
0.40	0.47	0.41	0.42	0.42	0.49	0.41	—	0.58
0.52	0.58	0.53	0.53	0.51	0.58	0.51	0.46	—
0.72	0.73	0.70	0.75	0.63	0.68	0.62	—	0.58
0.89	0.95	0.94	0.93	0.65	0.69	0.63	0.62	—
				0.71	0.71	0.66	0.70	—
				0.79	0.79	0.76	0.80	—
				0.81	0.82	0.80	—	0.65
				0.90	0.98	0.98	0.91	—

Note: Model-predicted activities according to (1) structure-energy model with ρ = 0.20 and no CFSE and (2) structure-energy model with ρ = 0.21 and CFSE. Experimental observations are after (3) Campbell and Roeder (1968), (4) Boström and Rosen (1988), and (5) Ottonello and Morlotti (1987).

ACKNOWLEDGMENTS

We wish to thank Dr. Don Boström of Umeå University, who very kindly supplied the crystals used for this experiment. We are grateful to M. A. Carpenter, G. P. Lumpkin, and G. Rossi for their reviews.

REFERENCES CITED

Baerlocher, Ch., Hepp, A., and Meier, W.M. (1977) A program for the simulation of crystal structures by geometric refinement. Institute of Crystallography and Petrography, ETH Zurich, Switzerland.

Berman, R.G., and Brown, T.H. (1985) Heat capacity of minerals in the system Na_2O-K_2O-CaO-MgO-FeO-Fe_2O_3-Al_2O_3-SiO_2-TiO_2-H_2O-CO_2: Representation, estimation, and high temperature extrapolation. Contributions to Mineralogy and Petrology, 89, 168–183.

Bish, D.L. (1981) Cation ordering in synthetic and natural Ni-Mg olivine. American Mineralogist, 66, 770–776.

Boström, D. (1987) Single-crystal X-ray diffraction studies of synthetic Ni-Mg olivine solid solutions. American Mineralogist, 72, 965–972.

Boström, D., and Rosen, E. (1988) Determination of activity-composition in $(Ni,Mg)_2SiO_4$ solid solution at 1200–1600 K by solid state emf measurements. Acta Chimica Scandinava, A42, 149–155.

Campbell, F.E., and Roeder, P. (1968) The stability of olivine and py-

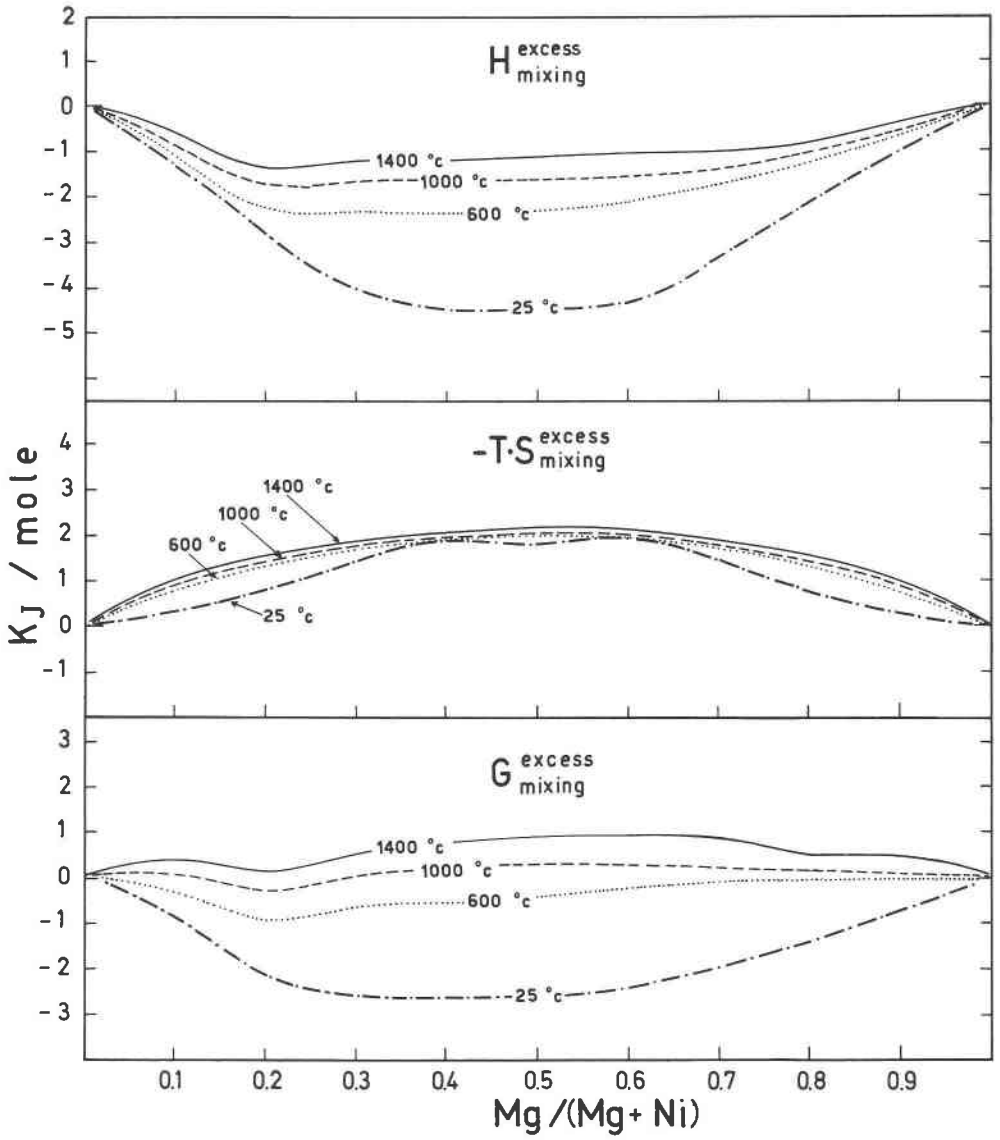

Fig. 3. Excess mixing properties for Ni-Mg mixture at various T conditions according to structure-energy model with $\rho = 0.21$ in presence of CFSE.

roxene in the Ni-Mg-Si-O system. American Mineralogist, 53, 257–268.

Catti, M. (1981) A generalized Born-Mayer parametrization of the lattice energy in orthorhombic ionic crystals. Acta Crystallographica, A37, 72–76.

Hamilton, W.C. (1959) On the isotropic temperature factor equivalent to a given anisotropic temperature factor. Acta Crystallographica, 12, 609–610.

Helgeson, H.C., Delany, J.M., Nesbitt, H.W., and Bird, D.K. (1978) Summary and critique of thermodynamic properties of rock-forming minerals. American Journal of Sciences, 278A, 1–229.

Lumpkin, G.R., and Ribbe, P.H. (1983) Composition, order-disorder and lattice parameters of olivines: Relationships in silicate, germanate, beryllate, phosphate, and borate olivines. American Mineralogist, 68, 164–176.

Matsui, Y., and Syono, Y. (1968) Unit cell dimensions of some synthetic olivine group solid solutions. Geochemical Journal, 2, 51–59.

Ottonello, G. (1987) Energies and interactions in binary (Pbnm) orthosilicates: A Born parametrization. Geochimica et Cosmochimica Acta, 51, 3119–3135.

Ottonello, G., and Morlotti, R. (1987) Thermodynamics of the (nickel + magnesium) olivine solid solution. Journal of Chemical Thermodynamics, 19, 809–818.

Rajamani, V., Brown, G.E., and Prewitt, C.T. (1975) Cation ordering in Ni-Mg olivine. American Mineralogist, 60, 292–299.

Robinson, K., Gibbs, G.V., and Ribbe, P.H. (1971) Quadratic elongation, a quantitative measure of distortion in coordination polyhedra. Science, 172, 567–570.

Seifert, S., and O'Neill, H.St.C. (1987) Experimental determination of activity-composition relations in Ni_2SiO_4-Mg_2SiO_4 and Co_2SiO_4-Mg_2SiO_4

olivine solid solutions at 1200 K and 0.1 MPa and 1573 K and 0.5 GPa. Geochimica et Cosmochimica Acta, 51, 97–104.

Shannon, R.D. (1976) Revised effective ionic radii and systematic studies of interatomic distances in halides and chalcogenides. Acta Crystallographica, A32, 751–767.

Tosi, M. (1964) Cohesion of ionic solids in the Born model. Solid State Physics, 16, 1–120.

Wood, B.J. (1974) Crystal field spectrum of Ni^{2+} in olivine. American Mineralogist, 59, 244–248.

Zachariasen, W.H. (1963) The secondary extinction correction. Acta Crystallographica, 16, 1139–1144.

Zemansky, M.W. (1957) Heat and thermodynamics. McGraw-Hill, New York.

Manuscript received November 6, 1987
Manuscript accepted October 31, 1988